UDC 531.383 DOI: 10.18698/1812-3368-2021-5-17-32

ANALYTICAL SOLUTION OF THE DYNAMICS EQUATIONS FOR A WAVE SOLID-STATE GYROSCOPE USING THE ANGULAR RATE LINEAR APPROXIMATION

M.A. Basarab[1] basarab@bmstu.ru
B.S. Lunin[2] lbs@kge.msu.ru
I.P. Ivanov[1] ivanov@bmstu.ru

[1] **Bauman Moscow State Technical University, Moscow, Russian Federation**
[2] **Lomonosov Moscow State University, Moscow, Russian Federation**

Abstract

The exact solution is provided of the dynamics equation for an elastic inextensible ring being the basic model of a wave solid-state gyroscope with the linear law of the base angular rotation rate alteration. This solution is presented in terms of the parabolic cylinder functions (Weber function). Asymptotic approximations are used in the device certain operating modes. On the basis of the solution obtained, the analytical solution to the equation of the ring dynamics in case of piecewise linear approximation of the angular rate arbitrary profile on a time grid is derived. This significantly expands the class of angular rate dependences, for which the solution could be written down analytically. Earlier, in addition to the simplest case of constant angular rate, solutions were obtained for angular rate varying according to the square root law with time (Airy function), as well as according to the harmonic law (Mathieu function). Error dependence of such approximation on the discretization step in time is estimated numerically. Results obtained make it possible to reduce the number of operations, when it is necessary to study long-term evolutions of the dynamic system oscillations, as well as to quantitatively and qualitatively control convergence of finite-difference schemes in solving dynamics equations for a wave solid-state gyroscope with the ring resonator

Keywords

Wave solid-state gyroscope, angular rate, Weber functions, piecewise linear approximation

Received 11.03.2021
Accepted 11.06.2021

Introduction. Wave solid-state gyroscope (WSSG) operation is based on the precession effect of elastic waves excited in the axisymmetric bodies [1–4]. As a rule, revolution shells (hemispherical WSSG — HRG [5], cylindrical

WSSG — CRG [6], etc.), as well as elastic ring resonators connected to the base through a system of suspensions (torsions) [7–9] are used as such bodies. Precession mechanism (Brian effect) is explained by exposure to the Coriolis force with the rotating shell or ring points performing a complex motion, i.e., relative oscillatory and transport motion with the Ω certain angular rate. The excited standing wave rotates in a plane perpendicular to the symmetry axis similar to a solid body demonstrating the inertial properties. At the same time, the wave rotation angle is less than the base rotation angle, which makes it possible to measure it and the angular rate Ω. The indicated effect is valid for any base variable rotation rate $\Omega = \Omega(t)$ [2].

Taking into account the fact that main portion of the elastic shell oscillation energy corresponds to the region adjacent to its edge, the ring model is the basic one in studying the WSSG dynamics of any configuration. Analysis of the ring resonator dynamics is especially simple in the case of constant angular rate ($\Omega = \text{const}$). For certain dependencies $\Omega(t)$, by reducing to the known differential equations of the second order with a variable coefficient for ring resonator, dynamics equation solutions could also be found analytically [2, 3]. First, the form of these solutions could be quite cumbersome (expressed in terms of special functions). Second, not every law of the base rotation enables to obtain well-studied analytically differential equations. In particular, this applies to such practically important cases, where the $\Omega(t)$ analytical dependence changes smoothly or abruptly over time, as well as if it is specified not analytically, but in a tabular form (an example of such WSSG use could be the task of monitoring the drill position in drilling oil and gas wells [10], when the drill rotates with the arbitrary high angular rate, including abruptly changing, and significantly exceeding the linear motion velocity).

In this regard, the numerical solution methods are mostly universal [7, 11]. One of the most significant disadvantages of numerical methods is the need to find a compromise between operation speed and accuracy of the difference schemes, i.e., the smaller is the grid step, the lower is the error, and at the same time, the higher is the computation volume when calculating dynamics at large intervals. Another disadvantage is the probable stability loss in such schemes, especially at large grid steps, and in cases of large-amplitude nonlinear coefficients in the original differential equations. In particular, this refers to the actual problem of simulating high-intensity dynamic processes, when an angular rate or an angular acceleration are characterized by high amplitudes [12, 13].

In order to preserve advantages of the analytical methods making it possible to quickly calculate motion parameters in any predetermined moment of time according to the given initial conditions, and at the same time to use universality of the numerical methods, this work proposes the following numerical-analytical method. Its essence lies in the piecewise linear approximation of an arbitrary dependence $\Omega(t)$ with the subsequent exact solution of problems on each segment, where $\mathrm{d}\Omega/\mathrm{d}t = \text{const}$. In this case, it is sufficient only to calculate linear displacement and acceleration values of the ring points at the end of the intervals, which are at the same time the initial conditions for subsequent segments.

Antinode real amplitude and phase should certainly be evaluated taking into account many various factors, including structure imperfection (resonator frequency splitting and different quality factors), nonlinearity in the material characteristics and their dependence on external factors (temperature, etc.), imperfection of the external excitation system, external vibrations, etc. Taking into account the interrelated influence of such factors requires the involvement of the predominantly numerical simulation apparatus based on the finite-difference method (FDM) and the finite-element method (FEM) [14, 15]. These computational experiments are a time-consuming procedure, especially when analyzing the WSSG dynamics over long-time intervals. At the same time, numerical methods when simulating the intense dynamic processes, could lead to significant errors and also demonstrate computational instability. Therefore, analytical solutions similar to the one proposed in this work could make it possible to assess the adequacy of finite-difference and finite-element schemes on the ideal resonator dynamics model in order to further investigate more complex cases using them.

Let us consider initially the case of analytical solution for the base linear angular rate, including situations requiring the use of asymptotic expansions. Further, these solutions are introduced as the basic in producing a general numerical-analytical solution for approximating the arbitrary angular rate. The numerical experiment demonstrates the proposed approach effectiveness.

Wave solid-state gyroscope operation principle. Standing wave with the k oscillation form number is excited in the elastic ring (resonator) of radius R with the finite cross-sectional area. The form of such a wave for $k = 2$ is shown in Fig. 1, the wave maxima points (antinodes) in the polar coordinate system associated with the device body are oriented at angle φ_0. Device body rotation with the angular rate Ω leads to the φ_k^* antinode orientation angle turn according to the following law:

$$\varphi_k^*(t) = \varphi_0 - \frac{2}{k^2+1}\int_0^t \Omega(s)\,\mathrm{d}s.$$

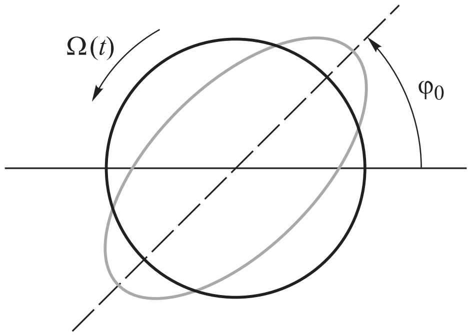

Fig. 1. Diagram illustrating the WSSG operation principle

Standing wave rotates around the base similarly to a solid body thus demonstrating the inertial properties. In this case, the standing wave rotation angle in space is less than the device body rotation angle, and with the φ_0 known, the $\varphi_k^*(t)$ angle serves as the base rotation angle value. The precession occurrence mechanism (Bryan effect) is explained by exposure to the Coriolis force, when the rotating elastic ring points are in a complex motion: relative oscillatory and transport with the angular rate Ω.

Mathematical model. Partial differential equation describing free oscillations dynamics in the elastic inextensible ring has the following dimensionless form [2–4]:

$$\frac{\partial^4 w}{\partial\varphi^2\partial\tau^2}-\frac{\partial^2 w}{\partial\tau^2}+4\Theta\frac{\partial^2 w}{\partial\varphi\partial\tau}-\Theta^2\left(\frac{\partial^4 w}{\partial\varphi^4}+3\frac{\partial^2 w}{\partial\varphi^2}\right)+$$
$$+2\frac{\partial\Theta}{\partial\tau}\frac{\partial w}{\partial\varphi}+\left(\frac{\partial^6 w}{\partial\varphi^6}+2\frac{\partial^4 w}{\partial\varphi^4}+\frac{\partial^2 w}{\partial\varphi^2}\right)=0, \qquad (1)$$

where $w(\varphi,\tau)$ is the ring point radial displacement depending on the polar angle φ and on the dimensionless time τ; $\Theta(\tau)$ is the dimensionless angular rate.

The transition from dimensionless to dimensional values is carried out using the following replacements for the variable time (t, s) and angular rate (Ω, rad/s):

$$t=\frac{\nu}{\omega}\tau;\qquad \Omega(t)=\frac{\omega}{\nu}\Theta\left(\frac{\omega}{\nu}t\right).$$

Here ω is the dimensional natural oscillation frequency depending on the material characteristics and the resonator geometry, rad/s; ν is the dimensionless natural oscillation frequency.

For the oscillation main second form in the elastic ring plane, the following is provided:

$$\nu = \frac{6}{\sqrt{5}}. \quad (2)$$

For an unambiguous solution (1), it is necessary to set initial conditions and periodicity conditions:

$$w(\varphi, \tau_0) = u_1(\varphi), \quad \frac{\partial w(\varphi, \tau_0)}{\partial \tau} = u_2(\varphi); \quad (3)$$

$$\frac{\partial^{(l)} w(0, \tau)}{\partial \varphi^l} = \frac{\partial^{(l)} w(2\pi, \tau)}{\partial \varphi^l}, \quad l = 0, \ldots, 5.$$

Solution (1) is of practical interest corresponding to the second form of ring oscillations with the natural frequency (2):

$$w(\varphi, \tau) = p(\tau)\cos 2\varphi + q(\tau)\sin 2\varphi. \quad (4)$$

Detailed analysis of the partial differential equation (1) making it possible to write down its general solution (4) in the following form:

$$w(\varphi, \tau) = (C_1 y_1 + C_2 y_2)\cos 2(\varphi - \gamma) + (C_3 y_1 + C_4 y_2)\sin 2(\varphi - \gamma), \quad (5)$$

is provided in [2, 3]. In (5) y_1, y_2 are the linearly independent solutions of the ordinary differential equation of the second order:

$$\frac{d^2 y}{d\tau^2} + \nu^2 \left(1 + \frac{1}{5}\Theta^2\right) y = 0; \quad (6)$$

C_1, C_2, C_3, C_4 are the coefficients found from the initial conditions (3); γ is the variable phase,

$$\gamma(\tau) = -\frac{2}{5}\int_{\tau_0}^{\tau} \Theta(z)\, d z. \quad (7)$$

Solution (1) should be found under an assumption that functions in the right-hand sides of the initial conditions (3) are representable in the form of the oscillation basic mode (4):

$$u_1(\varphi) = A_1 \cos 2\varphi + B_1 \sin 2\varphi; \quad u_2(\varphi) = A_2 \cos 2\varphi + B_2 \sin 2\varphi, \quad (8)$$

and the rest of their expansion harmonics in the Fourier series could be neglected.

Expressions (8) could also be written in the same way as

$$u_1(\varphi) = \Lambda_1 \cos 2(\varphi - \varphi_0), \quad u_2(\varphi) = \Lambda_2 \cos 2(\varphi - \varphi_0'),$$

where Λ_1, Λ_2 and φ_0, φ_0' are the specified amplitudes and phases. Then

$$A_1 = \Lambda_1 \cos 2\varphi_0, \; B_1 = \Lambda_1 \sin 2\varphi_0, \; A_2 = \Lambda_2 \cos 2\varphi_0', \; B_2 = \Lambda_2 \sin 2\varphi_0',$$

and obviously

$$A_i = \frac{1}{\pi}\int_0^{2\pi} u_i(\varphi)\cos 2\varphi \, d\,\varphi, \;\; B_i = \frac{1}{\pi}\int_0^{2\pi} u_i(\varphi)\sin 2\varphi \, d\,\varphi, \;\; i = 1, \;\; 2.$$

Given that

$$\gamma(\tau_0) = 0, \;\; \left.\frac{d\gamma}{d\tau}\right|_{\tau=\tau_0} = -\frac{2}{5}\Theta(\tau_0),$$

to determine the $C_1, C_2, C_3, C_4,$ the following linear algebraic equations system is obtained:

$$\begin{gathered}
\left.(C_1 y_1 + C_2 y_2)\right|_{\tau=\tau_0} = A_1, \\
\left.\left(C_1\frac{dy_1}{d\tau} + C_2\frac{dy_2}{d\tau} + \frac{4}{5}(C_3 y_1 + C_4 y_2)\Theta\right)\right|_{\tau=\tau_0} = A_2; \\
\left.(C_3 y_1 + C_4 y_2)\right|_{\tau=\tau_0} = B_1, \\
\left.\left(-\frac{4}{5}(C_1 y_1 + C_2 y_2)\Theta + C_3\frac{dy_1}{d\tau} + C_4\frac{dy_2}{d\tau}\right)\right|_{\tau=\tau_0} = B_2.
\end{gathered} \qquad (9)$$

Solution (9) has the following form:

$$\begin{aligned}
C_1 &= \left.\left[y_1\frac{d\,y_2}{d\,\tau} - y_2\frac{d\,y_1}{d\,\tau}\right]^{-1}\left[A_1\frac{d\,y_2}{d\,\tau} - y_2\left(A_2 - B_1\frac{4}{5}\Theta\right)\right]\right|_{\tau=\tau_0}; \\
C_2 &= \left.\left[y_1\frac{d\,y_2}{d\,\tau} - y_2\frac{d\,y_1}{d\,\tau}\right]^{-1}\left[y_1\left(A_2 - B_1\frac{4}{5}\Theta\right) - A_1\frac{d\,y_1}{d\,\tau}\right]\right|_{\tau=\tau_0}; \\
C_3 &= \left.\left[y_1\frac{d\,y_2}{d\,\tau} - y_2\frac{d\,y_1}{d\,\tau}\right]^{-1}\left[B_1\frac{d\,y_2}{d\,\tau} - y_2\left(B_2 + A_1\frac{4}{5}\Theta\right)\right]\right|_{\tau=\tau_0}; \\
C_4 &= \left.\left[y_1\frac{d\,y_2}{d\,\tau} - y_2\frac{d\,y_1}{d\,\tau}\right]^{-1}\left[y_1\left(B_2 + A_1\frac{4}{5}\Theta\right) - B_1\frac{d\,y_1}{d\,\tau}\right]\right|_{\tau=\tau_0}.
\end{aligned} \qquad (10)$$

Equation (6) admits an exact solution for certain types of dependencies of practical interest $\Theta = \Theta(\tau)$, in particular:

1) $\Theta = \Theta_0 = \text{const}$ (y_1, y_2 are trigonometric functions);

2) $\Theta(\tau) = \sqrt{a\tau}$ or $\Theta(\tau) = \sqrt{\Theta_0^2 - a\tau}$, where $a = \text{const} > 0$ (y_1, y_2 are Airy functions);

3) $\Theta(\tau) = \Theta_0 \sin \lambda\tau$ (y_1, y_2 are written by means of periodic Mathieu functions).

It was noted [2, 3] that with the linear dependence

$$\Theta(\tau) = c\tau + b \tag{11}$$

the y_1, y_2 solutions could be expressed in terms of the parabolic cylinder functions [16].

It should be noted that dependence (11) is of particular interest due to the fact that the simplest continuous approximation of sufficiently arbitrary dependence $\Theta = \Theta(\tau)$ is possible using the piecewise linear representation. In this connection, let us consider in more the detail solution for linear dependence (11), after that let us present the general algorithm for finding an analytical solution to the equation of the elastic inextensible ring dynamics in the case of the angular rate arbitrary piecewise linear dependence on time.

Analytical solution at the angular rate linear law. Substituting (11) into (6), the following is obtained:

$$\frac{\mathrm{d}^2 y}{\mathrm{d}\tau^2} + \nu^2 \left[1 + \frac{1}{5}(c\tau + b)^2 \right] y = 0. \tag{12}$$

Using the linear change of variable $\tau = gx + d$, where $g = \sqrt{5/(12c)}$, $d = -b/c$, let us reduce (12) to a standard form of the Weber equation for functions of the parabolic cylinder [16]:

$$\frac{\mathrm{d}^2 y}{\mathrm{d}x^2} + \left(\frac{1}{4}x^2 - \mu \right) y = 0, \tag{13}$$

where $\mu = -3/c$.

It should be noted that the indicated replacement is correct for any sign of the c coefficient (angular rate), despite the fact that g would be imaginary for $c < 0$.

Even and odd linearly independent solutions of equation (13) have the following form [16]:

$$y_1(\mu, x) = \sum_{k=0}^{\infty} a(\mu)_{2k} \frac{x^{2k}}{(2k)!}, \quad y_2(\mu, x) = \sum_{k=0}^{\infty} a(\mu)_{2k+1} \frac{x^{2k+1}}{(2k+1)!}, \tag{14}$$

where

$$a(\mu)_0 = a(\mu)_1 = 1, \quad a(\mu)_{n+2} = \mu a(\mu)_n - \frac{1}{4} n(n-1) a(\mu)_{n-2}, \ n = 2, 3, \ldots$$

With high time values ($\tau \to \infty$) or angular velocity low values ($|c| \to 0$). it is necessary to keep a sufficiently large number of terms of the significantly oscillating infinite power series (14). In this regard, asymptotic representations should be used.

Let us introduce the following notation:

$$X = \sqrt{x^2 - 4\mu} = 2\sqrt{\frac{3}{c}\left[1 + \frac{(t+b)^2}{5}\right]}.$$

In most cases of practical importance, the following Darwin expansions [16] are suitable in the fast-enough representations.

1. Long time, low angular velocity $(x^2 \gg 4\mu)$:

$$y_1(\mu, x) = \operatorname{Re} E(\mu, x), \qquad y_2(\mu, x) = \operatorname{Im} E(\mu, x),$$
$$E(\mu, x) = \sqrt{2}\exp\left(v_r(\mu, x) + i\left[\frac{\pi}{4} + \theta_1(\mu, x) + v_i(\mu, x)\right]\right),$$
$$\theta_1(\mu, x) = \begin{cases} \dfrac{1}{4}xX - \mu\,\mathrm{arch}\,\dfrac{x}{2\sqrt{\mu}}, & \mu > 0 \quad (c < 0), \\ \dfrac{1}{4}xX - \mu\,\mathrm{arsh}\,\dfrac{x}{2\sqrt{|\mu|}}, & \mu < 0 \quad (c > 0). \end{cases} \tag{15}$$

2. Low time, high angular velocity $(x^2 \ll 4\mu,\ \mu > 0)$:

$$y_1(\mu, x) = \frac{1}{\sqrt{\kappa}}\exp\left[-\theta(\mu, x) + v(\mu, x)\right],$$
$$y_2(\mu, x) = \sqrt{\kappa}\exp\left[\theta(\mu, x) + v(\mu, -x)\right], \tag{16}$$
$$\theta(\mu, x) = \frac{1}{4}ixX + \mu\arcsin\frac{x}{2\sqrt{\mu}}, \qquad \kappa = \sqrt{1 + \mathrm{e}^{2\pi\mu}} - \mathrm{e}^{\pi\mu}.$$

In (15), (16):

$$v_r(\mu, x) = -\frac{1}{2}\ln X - \frac{\delta_6}{X^6} + \frac{\delta_{12}}{X^{12}} - \ldots, \qquad v_i(\mu, x) = -\frac{\delta_3}{X^3} + \frac{\delta_9}{X^9} - \frac{\delta_{15}}{X^{15}} + \ldots,$$
$$v(\mu, x) = -\frac{1}{2}\ln|X| + \frac{\delta_3}{|X|^3} + \frac{\delta_6}{|X|^6} + \frac{\delta_9}{|X|^9}\ldots,$$

and expressions for the certain initial coefficients δ_{3k} are

$$\delta_3 = -\frac{1}{\mu}\left(\frac{x^2}{48} - \frac{1}{2}\mu x\right), \qquad \delta_6 = \frac{3}{4}x^2 + 2\mu,$$
$$\delta_9 = \frac{1}{\mu^3}\left(\frac{7}{5760}x^9 - \frac{7}{320}\mu x^7 + \frac{49}{320}\mu^2 x^5 + \frac{31}{12}\mu^3 x^3 + 19\mu^4 x\right),$$
$$\delta_{12} = \frac{153}{8}x^4 + 186\mu x^2 + 80\mu^2.$$

The variable phase (7) is equal to

$$\gamma(\tau) = -\frac{2}{5}(\tau - \tau_0)\left(\frac{c}{2}(\tau + \tau_0) + b\right).$$

The final solution to the problem (1) is written down as:

$$w(\varphi, \tau) = \left[C_1 y_1(\mu, x) + C_2 y_2(\mu, x)\right] \cos 2(\varphi - \gamma) +$$

$$+\left[C_3 y_1(\mu, x) + C_4 y_2(\mu, x)\right] \sin 2(\varphi - \gamma), \qquad (17)$$

where $x = (\tau - d) / g$, and undefined coefficients are found according to (10).

Derivatives of the y_1, y_2 functions in (10) could be calculated analytically, for example, by the term-by-term differentiation of series (14).

Analytical solution for piecewise linear approximation of the angular rate. Let the base angular rate be $\Theta(\tau) \in C[\tau_0, T]$. At the $\tau \in [\tau_0, T]$ interval, the uniform grid is introduced:

$$j = 0,\ 1, \ldots, N,\ \ h = \frac{T - \tau_0}{N},\ \ \tau_j = \tau_0 + jh,\ \ \Theta_j = \Theta(\tau_j).$$

Let us approximate the $\Theta(\tau)$ dependence using the piecewise linear interpolation

$$\tilde{\Theta}(\tau) = \sum_{j=0}^{N} \Theta_j B_1\left(\frac{\tau}{h} - j\right), \qquad (18)$$

with the following Schoenberg linear splines [17]:

$$B_1(z) = \begin{cases} 1 - |z|, & |z| \le 1, \\ 0, & |z| \ge 1. \end{cases}$$

Moreover, it could be noted that for $\tau \in [\tau_j, \tau_{j+1}]$

$$\tilde{\Theta}(\tau) = c_j \tau + b_j,\ \ j = 0,\ 1, \ldots, N - 1, \qquad (19)$$

where

$$c_j = \frac{1}{h}\left(\Theta_{j+1} - \Theta_j\right),\ \ b_j = \frac{1}{h}\left(\Theta_j \tau_{j+1} - \Theta_{j+1} \tau_j\right).$$

The proposed algorithm is designed to recursively obtain a solution to the elastic ring dynamics equation (1) with linear angular rate (19) at each subinterval $[\tau_j, \tau_{j+1}]$. Initial conditions are used at the $[\tau_0, \tau_1]$ starting subinterval (4). And it is necessary to use the values $\mathrm{d}\, w(\varphi, \tau_j) / \mathrm{d}\, \tau$, calculated in the $[\tau_{j-1}, \tau_j]$ previous subinterval to identify initial conditions at each subsequent subinterval

$[\tau_j, \tau_{j+1}],\ j = 1, \ldots, N-1.$ In this case, the derivative expression has the following form:

$$\left.\frac{\mathrm{d}\,w}{\mathrm{d}\,\tau}\right|_{\tau=\tau_j} = \left[\left(C_1 \frac{\mathrm{d}\,y_1}{\mathrm{d}\,\tau} + C_2 \frac{\mathrm{d}\,y_2}{\mathrm{d}\,\tau} - 2\,(C_3 y_1 + C_4 y_2)\frac{\mathrm{d}\,\gamma}{\mathrm{d}\,\tau}\right)\cos 2\,(\varphi-\gamma) + \right.$$
$$\left.\left. + \left[C_3 \frac{\mathrm{d}\,y_1}{\mathrm{d}\,\tau} + C_4 \frac{\mathrm{d}\,y_1}{\mathrm{d}\,\tau} + 2(C_1 y_1 + C_2 y_2)\frac{\mathrm{d}\,\gamma}{\mathrm{d}\,\tau}\right]\sin 2\,(\varphi-\gamma)\right]\right|_{\tau=\tau_j},$$

where

$$\left.\frac{\mathrm{d}\,\gamma}{\mathrm{d}\,\tau}\right|_{\tau=\tau_j} = -\frac{2}{5}(c_j \tau_j + b_j).$$

Numerical experiment. If the $\Theta(\tau)$ angular velocity dependence is initially piecewise linear, then an exact solution by the Weber function could be obtained by correspondingly choosing the non-uniform approximation grid with nodes $\tau_j,\ j = 0,\ 1, \ldots, N.$ At the same time, the simplest analytical solution expressed by trigonometric functions should be used in the sections with constant angular rate, and in the angular acceleration nonzero sections — representation in terms of the parabolic cylinder functions (17), expressed depending on the acceleration sign and its absolute value, as well as on the time interval length in terms of power series (14), or one of the Darwin expansions (15), (16).

Example 1. Let us consider a case [2, 3, 11], where the angular rate changes according to the law $\Theta(\tau) = \sqrt{\tau}.$ Boundary conditions (3) are taken in the following form:

$$w(\varphi, \tau_0) = u_1(\varphi) = A_1 \cos 2\varphi + B_1 \sin 2\varphi, \qquad \frac{\partial w(\varphi, \tau_0)}{\partial \tau} = u_2(\varphi) = 0, \qquad (20)$$

where $\tau_0 = 0,\ A_1 = 1,\ B_1 = 0.$

Analytical solution (7) should be written as follows:

$$w(\varphi, \tau) = \left[C_1\ \mathrm{Ai}(-\theta) + C_2\ \mathrm{Bi}(-\theta)\right]\cos 2\left(\varphi + \frac{4}{15}\tau^{3/2}\right), \qquad (21)$$

where $\mathrm{Ai},\ \ \mathrm{Bi}$ are the Airy functions [16]; $\theta(\tau) = \nu^{3/2}(1+\tau);$

$$C_1 = A_1 \frac{\mathrm{Bi}'_\theta(-\nu^{3/2})}{\mathrm{Ai}(-\nu^{3/2})\,\mathrm{Bi}'_\theta(-\nu^{3/2}) - \mathrm{Bi}(-\nu^{3/2})\,\mathrm{Ai}'_\theta(-\nu^{3/2})};$$

$$C_2 = -A_1 \frac{\mathrm{Ai}'_\theta(-\omega^{3/2})}{\mathrm{Ai}(-\nu^{3/2})\,\mathrm{Bi}'_\theta(-\nu^{3/2}) - \mathrm{Bi}(-\nu^{3/2})\,\mathrm{Ai}'_\theta(-\nu^{3/2})}.$$

Let us fix a sufficiently large time interval $T = 10$. Values of the ε relative root-mean-square error at the $\varphi_0 = 0$ resonator point for various parameters of the h approximation step are provided in Fig. 2. The error was estimated by the formula

$$\varepsilon = \sqrt{\frac{\int\limits_{\tau_0}^{T} \left[w(\varphi_0, \tau) - \tilde{w}(\varphi_0, \tau) \right]^2 \mathrm{d}\tau}{\int\limits_{\tau_0}^{T} w^2(\varphi_0, \tau)\, \mathrm{d}\tau}} \qquad (22)$$

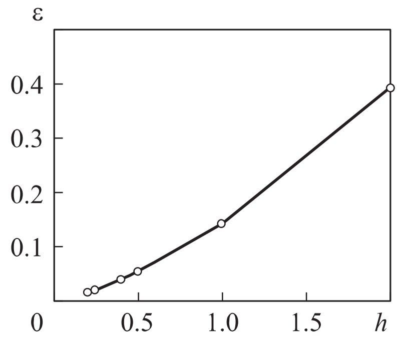

Fig. 2. The ε solution error dependence on the h step

using the Simpson quadrature formula on the uniform grid of 1000 nodes. In (22) w is the analytical solution (21); $\tilde{w}$ is the numerical-analytical solution obtained by piecewise-linear approximation of the $\Theta(\tau)$ dependence using the Darwin expansion (14).

Graphs of analytical solution and numerical-analytical solution at $h = 1$ are presented in Fig. 3.

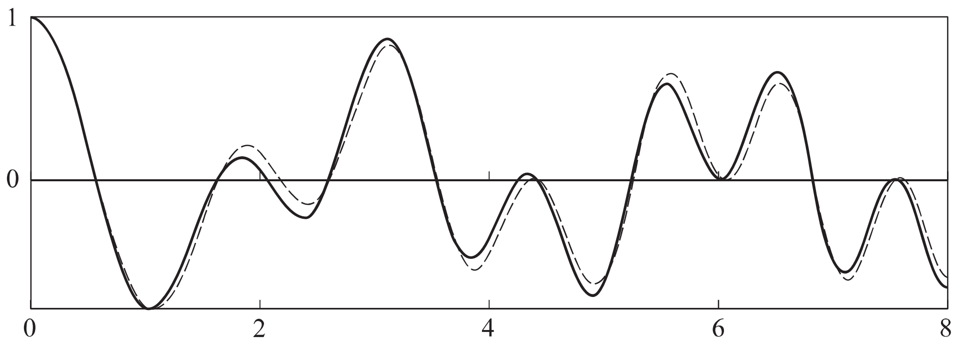

Fig. 3. Analytical (solid line) and numerical-analytical (dashed line) solutions (approximation step $h = 1$)

In accordance with Example 1, a relatively small approximate solution error for the $\Theta(\tau)$ smooth function is provided even on sufficiently coarse grids. When using the asymptotic Darwin expansions, the error is not increasing with the rising interval length; besides, high performance is provided with both, as compared to expansions in the form of power series (14), and in the finite-difference schemes. At the same time, analytical solution (21) required a cumbersome expression of the Airy functions and their derivatives in terms of the Bessel functions for fractional index, which in turn are represented in the form of infinite series, as well as of asymptotic expansions. In this sense, solutions of the dynamics equation for linear dependence of the angular rate and of the angular rate varying according to the square root law are to a certain equivalent. However, the obtained analytical solution in the first case could be extended to a more general situation, since universal representation in the form of linear B-splines (18) is widespread in the approximation theory.

Example 2. Let us consider the dynamics of the WSSG ring model free oscillations having an ideal metal cylindrical resonator and designed similar to the *InnaLabs*® devices [18] with the second form natural frequency of $\omega = 24510$ rad/s (3901 Hz) at the $t \in [0, T]$ in the dimensional mode.

The angular rate alteration law has the following form:

$$\Omega(t) = \begin{cases} 2\pi V t & t = 0, \ldots, 0.5T, \\ 2\pi V \cdot 0.5T & t = 0.5T, \ldots, T. \end{cases} \quad (23)$$

Expression (23) represents a model of the WSSG base rotation angular transfer to the stationary mode according to the linear law with the V, s^{-2}, angular acceleration.

Dependence piecewise linear approximation (23) proposes an exact analytical solution, if a grid is selected consisting of only three nodes:

$$j = 0,\ 1,\ 2,\ \Delta = \frac{T}{2},\ t_j = j\Delta\ (t_2 = T),$$
$$\Omega_0 = 0,\ \Omega_1 = \Omega_2 = \pi V T,$$

where similar to the dimensionless case $\Omega_j = \Omega(t_j)$. In this case, it is necessary in the $[t_0,\ t_1]$ segment with the linearly increasing angular rate to use a representation in the form of Weber functions asymptotic expansion according to the Darwin formulas (15). Next, new initial conditions are found at the t_1 point, after that analytical solution is written in terms of trigonometric functions in the $[t_1, t_2]$ section with constant angular rate:

$$w(\varphi, t) = (C_1 \cos\tilde{\omega}t + C_2 \sin\tilde{\omega}t)\cos 2(\varphi - \gamma) +$$
$$+ (C_3 \cos\tilde{\omega}t + C_4 \sin\tilde{\omega}t)\sin 2(\varphi - \gamma), \quad (24)$$

where

$$\tilde{\omega} = \sqrt{\omega^2 + \frac{36}{25}\Omega_1^2};\ \ \gamma(t) = -\frac{2}{5}\Omega_1(t - t_1). \quad (25)$$

With initial excitation in the form of (14) with $A_1 = 10$ μm, $B_1 = 0$ at $T =$ $= 100$ ms, $V = 500$ s^{-2}, solution graphs for two different points corresponding to the antinode and the node at the initial time moment are presented in Fig. 4.

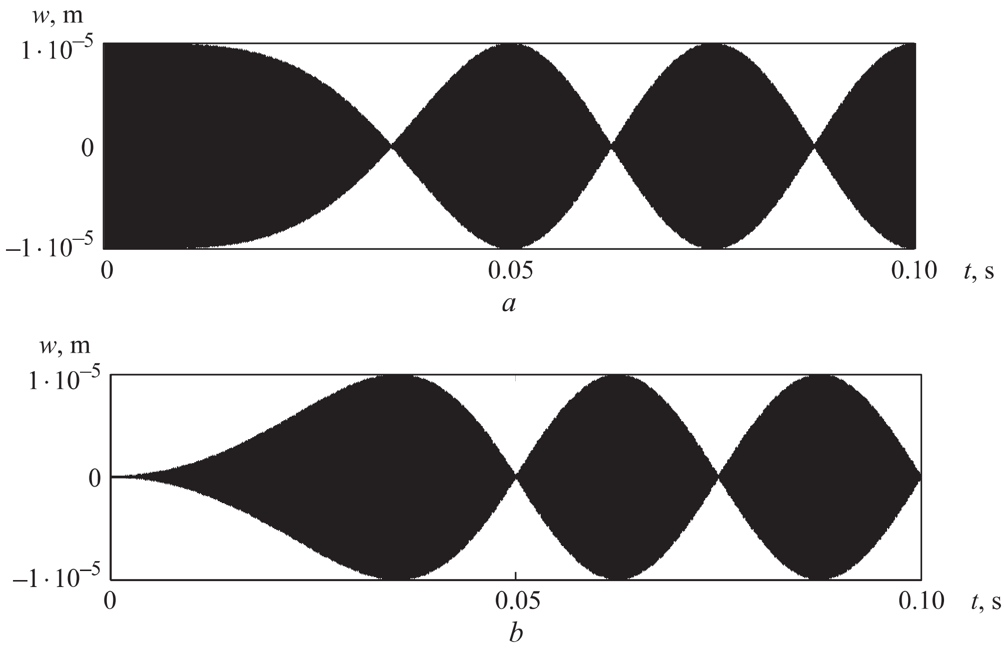

Fig. 4. Solution for dependence exact piecewise-linear approximation (23) at resonator points $\varphi = 0$ (*a*) and $\varphi = \pi/4$ (*b*)

Let us compare the obtained solution with the analytical solution found under the assumption that centrifugal forces could be neglected ($\Omega^2 = \Theta^2 = 0$). Omitting the corresponding terms in (1), (6) under the similar initial conditions the following expression is obtained:

$$w(\varphi, t) = A_1 \cos \omega t \cos 2\left(\varphi + \frac{2}{5}\int_0^t \Omega(z)\, dz\right). \tag{26}$$

Values of the solution relative root-mean-square error (26) similar to (16) in comparison with the exact analytical solution at different values of the angular acceleration V at the T = 100 ms interval are given in the Table. It should be noted that the error in oscillations (26) at the φ, $\varphi + \pi/4$ points is approximately equal to $\sqrt{2}$. Thus, Example 2 demonstrates that transferring to the mode with angular rates higher than 150 rad/s (angular rate reaching the values two orders of magnitude lower than the native angular frequency) and neglecting the centrifugal forces acting on the resonator points leads to errors of the order of several percent in comparison with the mismatch in the antiphase oscillations. The error is increasing by about an order of magnitude with the Ω_{max} rise by 3 times, which could be significant in designing the precision instruments.

Relative root-mean-square error values of the approximate solution (26) depending on dynamic parameters

V, s^{-2}	500	1000	1500	2000	2500	3000	3500	4000	4500	5000
Ω_{max}, rad/s	157	314	471	628	785	942	1100	1257	1414	1571
Ω_{max} / ω	0.006	0.013	0.019	0.026	0.032	0.038	0.045	0.051	0.058	0.064
ε	0.023	0.087	0.196	0.347	0.533	0.741	0.948	1.123	1.233	1.252

Conclusion. The proposed method, based on piecewise-linear approximation of the ring WSSG base rotation arbitrary angular rate makes it possible to obtain a recurrent sequence of analytical solutions on each linear segment by recalculating the initial conditions. Thus, a relatively narrow class of analytical solutions could be significantly expanded. Compared to numerical (finite-difference) solutions, the new method has high speed of response, which makes it possible to accurately simulate dynamics of oscillations over large time intervals without accumulating errors. Using the piecewise-linear approximation method allows studying accuracy and convergence of various finite-difference schemes. Using the suitable asymptotic expansions, it becomes possible to study dynamic processes of both very low and high intensity [12, 13]. The algorithm would be especially efficient with approximating on an uneven grid, when its step is smaller in the sections with significant alteration in the angular rate (high angular accelerations) and larger in relatively smooth areas. The resulting model could be particularly used to analyze the WSSG output signals when working with any $\Omega(t)$ dependence and to develop adequate requirements to the control electronics at the device design phase [19].

REFERENCES

[1] Bryan G.H. On the beats in the vibrations of a revolving cylinder or bell. *Proc. Camb. Phil. Soc. Math. Phys. Sci.*, 1890, vol. 7, pp. 101–111.

[2] Zhuravlev V.F., Klimov D.M. Volnovoy tverdotel’nyy giroskop [Solid-state wave gyroscope]. Moscow, Nauka Publ., 1985.

[3] Klimov D.M., Zhuravlev V.F., Zhbanov Yu.K. Kvartsevyy polusfericheskiy rezonator (volnovoy tverdotel’nyy giroskop) [Quartz hemisphere resonator (solid-state wave gyroscope)]. Moscow, Kim L.A. Publ., 2017.

[4] Lunin B.S., Matveev V.A., Basarab M.A. Volnovoy tverdotel’nyy giroskop. Teoriya i tekhnologiya [Solid-state wave gyroscope. Theory and technology]. Moscow, Radiotekhnika Publ., 2014.

[5] Deleye F. *SpaceNaute®* the HRG based inertial reference system of Ariane 6 European space launcher. *Gyroscopy Navig.*, 2019, vol. 10, no. 1, pp. 1–6.
DOI: https://doi.org/10.1134/S2075108719010036

[6] Basarab M.A., Lunin B.S., Matveev V.A., et al. Static balancing of cylindrical resonators of solid-state wave gyroscopes. *Giroskopiya i navigatsiya*, 2014, vol. 85, no. 2, pp. 43–51 (in Russ.).

[7] Ayazi F., Najafi K. A HARPSS polysilicon vibrating ring gyroscope. *J. Microelectromech. Syst.*, 2001, vol. 10, iss. 2, pp. 169–179. DOI: https://doi.org/10.1109/84.925732

[8] Liang D.-D., Yang X.-D., Zhang W., et al. Linear, nonlinear dynamics, and sensitivity analysis of a vibratory ring gyroscope. *Theor. Appl. Mech. Lett.*, 2018, vol. 8, iss. 6, pp. 393–403. DOI: https://doi.org/10.1016/j.taml.2018.06.001

[9] Huang D., Tang L., Cao R. Free vibration analysis of planar rotating rings by wave propagation. *J. Sound Vib.*, 2013, vol. 332, iss. 30, pp. 4979–4997.
DOI: https://doi.org/10.1016/j.jsv.2013.04.019

[10] Rozelle D.M. The hemispherical resonator gyro: from wineglass to the planets. *Proc. 19th AAS/AIAA Space Flight Mechanics Meeting*, 2009, pp. 1157–1178.

[11] Basarab M.A., Lunin B.S., Kolesnikov A.V. Numerical-analytical solution of the differential equation of free oscillations of an elastic ring when an arbitrary law of rotation of the basement. *Dinamika slozhnykh sistem — XXI vek* [Dynamics of Complex Systems — XXI Century], 2020, no. 2, pp. 5–15 (in Russ.).
DOI: https://doi.org/10.18127/j19997493-202002-01

[12] Basarab M., Lunin B., Vakhlyarskiy D., et al. Investigation of nonlinear high-intensity dynamic processes in a non-ideal solid-state wave gyroscope resonator. *Proc. 27th ICINS*, 2020, art. 9133943.
DOI: https://doi.org/10.23919/ICINS43215.2020.9133943

[13] Cooley C.G., Parker R.G. Vibration of high-speed rotating rings coupled to space-fixed stiffnesses. *J. Sound Vib.*, 2014, vol. 333, iss. 12, pp. 2631–2648.
DOI: https://doi.org/10.1016/j.jsv.2014.01.005

[14] Naraykin O.S., Sorokin F.D., Kozubnyak S.A., et al. Numerical simulation of elastic wave precession in the cylindrical resonator of a hemispherical resonator gyroscope featuring a non-homogeneous density distribution. *Herald of the Bauman Moscow State Technical University, Series Mechanical Engineering*, 2017, no. 5 (116), pp. 41–51 (in Russ.). DOI: https://doi.org/10.18698/0236-3941-2017-5-41-51

[15] Vakhlyarskiy D.S., Guskov A.M., Basarab M.A., et al. Using a combination of fem and perturbation method in frequency split calculation of a nearly axisymmetric shell with middle surface shape defect. *Nauka i obrazovanie: nauchnoe izdanie* [Science and Education: Scientific Publication], 2016, no. 5 (in Russ.). DOI: 10.7463/0516.0839190

[16] Abramowitz M., Stegun I.A., eds. Handbook of mathematical functions with formulas, graphs, and mathematical tables. New York, Dover, 1972.

[17] de Boor C. A practical guide to splines. Springer, 1978.

[18] InnaLabs: *website*. Available at: http://www.innalabs.com (accessed: 14.05.2021).

[19] Chumankin E.A., Basarab M.A., Matveev V.A., et al. Increase of the measurement range of the solid-state wave gyro with metallic resonator. *Pribory i sistemy. Upravlenie,*

kontrol', diagnostika [Instruments and Systems: Monitoring, Control, and Diagnostics], 2016, no. 10, pp. 25–37 (in Russ.).

Basarab M.A. — Dr. Sc. (Phys.-Math.), Assoc. Professor, Head of the Department of Information Security, Bauman Moscow State Technical University (2-ya Baumanskaya ul. 5, str. 1, Moscow, 105005 Russian Federation).

Lunin B.S. — Dr. Sc. (Eng.), Leading Researcher, Department of Chemistry, Lomonosov Moscow State University (Leninskie Gory 1/3, Moscow, 119991 Russian Federation).

Ivanov I.P. — Dr. Sc. (Eng.), Assoc. Professor, Head of the Department of Theoretical Informatics and Computer Technologies, Bauman Moscow State Technical University (2-ya Baumanskaya ul. 5, str. 1, Moscow, 105005 Russian Federation).

Please cite this article as:

Basarab M.A., Lunin B.S., Ivanov I.P. Analytical solution of the dynamics equations for a wave solid-state gyroscope using the angular rate linear approximation. *Herald of the Bauman Moscow State Technical University, Series Natural Sciences*, 2021, no. 5 (98), pp. 17–32. DOI: https://doi.org/10.18698/1812-3368-2021-5-17-32